Numerical Calibrations of an Analytical Generic Nuclear Repository Heat Transfer Model

American Nuclear Society Summer Meeting 2012

Kathryn D. Huff[1,2] & Theodore H. Bauer[2]

[1]University of Wisconsin-Madison & [2]Argonne National Laboratory

June 27, 2012

Outline

Future Disposal System Options

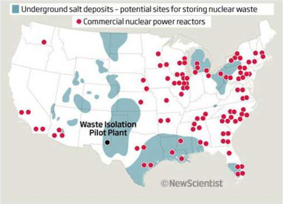

Figure: U.S. Salt Deposits, ref. [13].

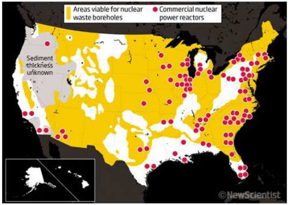

Figure: U.S. Crystalline Basement, ref. [13].

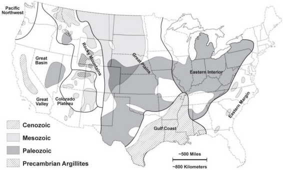

Figure: U.S. Clay Deposits, ref. [6].

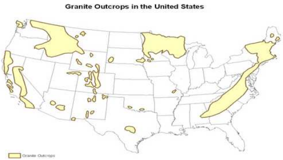

Figure: U.S. Granite Beds, ref. [3].

Future Fuel Cycle Options

Domestic Fuel Cycle Options

Title	Description	Challenges
Open	Once Through Current US PWR Fleet No Separations No Recycling Higher Burnups	High Temperatures, Volumes
Modified Open	Partial Recycling Next Gen. PWR Fleet Limited Separations Limited Transmutation Advanced Fuel Forms HLW treatment	Both high volumes and myriad fuel streams
Closed	Full Recycling Full Separations Full Recycling VHTGR, SFRs, other transmutation HLW treatment	Myriad fuel streams

Table: Domestic Fuel Cycle Options

Clay Disposal Environments

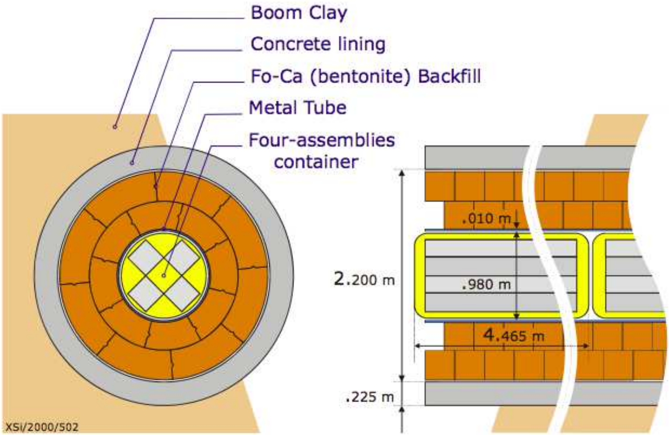

Figure: Belgian reference concept in Boom Clay [18].

Granite Disposal Environments

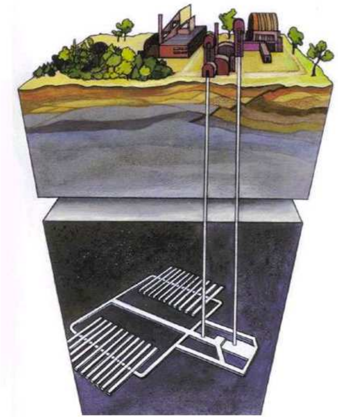

Figure: Czech reference concept in Granite [18].

Salt Disposal Environments

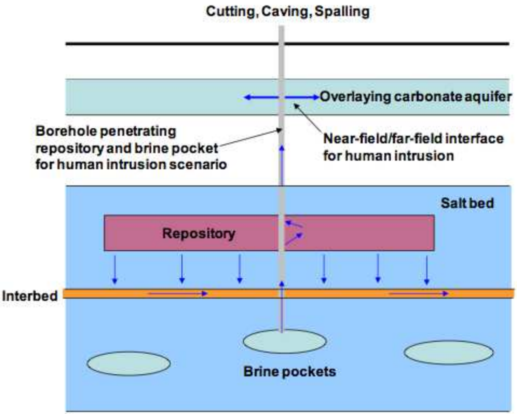

Figure: DOE-NE Used Fuel Disposition Campaign concept in Salt [5].

Deep Borehole Disposal Environment

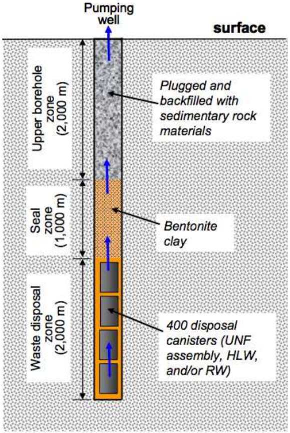

Figure: DOE-NE Used Fuel Disposition Campaign Deep Borehole concept [5].

Repository Layouts

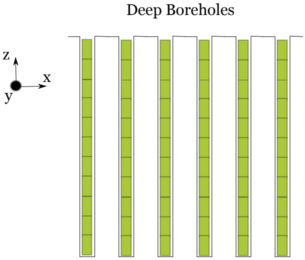

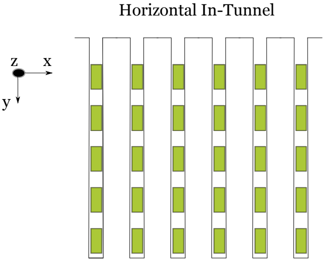

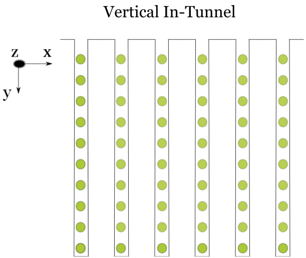

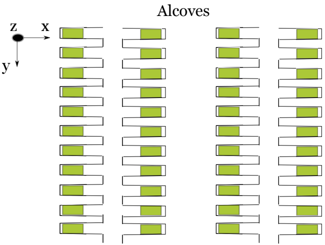

Methods of Heat Transport in Various Geologies

Models of Heat Load for Various Geologies

Source (Who)	Nation (Where)	Geology (What)	Methodology (How)
Enresa [18]	Spain	Granite	CODE_BRIGHT 3D Finite Element
NRI [18]	Czech Rep.	Granite	Specific Temperature Integral
ANDRA [2]	France	Granite	3D Finite Element CGM code
SKB [11]	Sweden	metagranite	1D-3D Site Descriptive Models
SCK·CEN [18]	Belgium	Clay	Specific Temperature Integral
ANDRA [1]	France	Argile Clay	3D Finite Element CGM code
NAGRA [9, 10]	Switzerland	Opalinus Clay	3D Finite Element CGM code
GRS [18]	Germany	Salt	HEATING (3D finite difference)
NCSU(Li) [12]	USA	Yucca Tuff	Specific Temperature Integral
NCSU(Nicholson) [14]	USA	Yucca Tuff	COSMOL 3D Finite Element
Radel & Wilson [16]	USA	Yucca Tuff	Specific Temperature Change

Table: Methods by which to calculate heat load are independent of geology. Maximum heat load constraints, however, vary among host formations.

Similar heat transport models can be used for all geologies, but are differentiated by material parameters (c_p, K, ρ), geometric parameters (tunnel spacing, tunnel radius), and different geochemical constraints.

Heat Limits In Various Geologies

Important heat limits in materials of the repository restrict loading designs and capacity.

Thermal Behavior of Various Concepts

Feature	Clay	Granite	Salt	Deep Borehole
Host Rock Limit [$^\circ C$]	~ 125	~ 200	~ 180	> 200
Buffer Limit [$^\circ C$]	100 (Fo-Ca)	100 (Fo-Ca)	180	100 (Fo-Ca)
Conductivity [$\frac{W}{m \cdot K}$]	$1-2$	$2-4$	~ 4	$2-4$
Diffusivity [$\frac{m^2}{s}$]	$1-6 \times 10^{-7}$	1×10^{-6}	$1-2 \times 10^{-6}$	1×10^{-6}
Coalesence	yes	no	yes	no

Table: Reference values for thermal limits and behaviors in various candidate repository geologies.

Impact of Repository Geologies

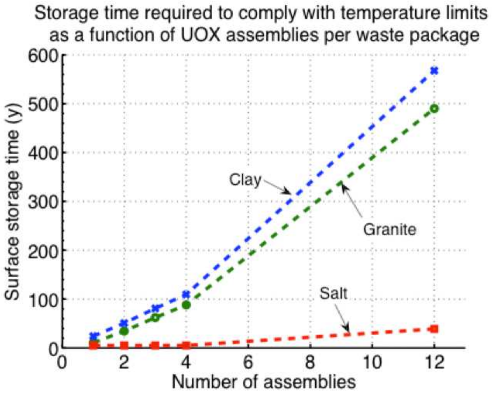

Figure H.6-1 Minimum surface storage time necessary to comply with waste package surface temperature limit as function of UOX assemblies per waste package in a granite, clay, and salt (with 75% of the waste package surface contacting intact salt) repository

Figure: LLNL has found that the higher heat limit, alcove geometry, and high conductivity in salt allows for earlier loading times.

Impact of Repository Designs

Yucca Mountain Footprint Expansion Calculations

Author	Max. Capacity *tonnes*	Footprint km^2	Details
OCRWM	70,000	4.65	"statutory case"
	97,000	6	"full inventory case"
	119,000	7	"additional case"
Yim, M.S.	75,187	4.6	SRTA code
	76,493	4.6	STI method
	95,970	4.6	63m drift spacing
	82,110	4.6	75 yrs. cooling
Nicholson, M.	103,600	4.6	drift spacing
EPRI			
	63,000	6.5	Base Case CSNF
option 1	126,000	13	expanded footprint
option 2	189,000	6.5	multi-level design
option 3	189,000	6.5	grouped drifts
options 2+3	252,000	6.5	hybrid
options 1+(2or3)	378,000	13	hybrid
options 1+2+3	567,000	13	hybrid

Table: Various analyses based on heat load limited repository designs have resulted in footprint expansion calculations of the YMR.

Abstraction For Systems Analysis

Figure: The LLNL analytical model is being used to generate a detailed dataset to support heat based repository capacity in a generic repository model plugin destined for the CYCLUS fuel cycle simulator (cyclus.github.com).

Outline

Analytical Model : Background

The analytical model

- was created at LLNL (H. Greenberg, J. Blink, et. al) [8, 17, 7]
- employs an analytic model from Carslaw and Jaeger [4]
- is implemented in MathCAD [15]
- seeks to inform heat limited waste capacity calculations for
  - arbitrary geology
  - arbitrary waste package loading densities
  - arbitrary homogeneous decay heat source

Analytical Model : Geometry

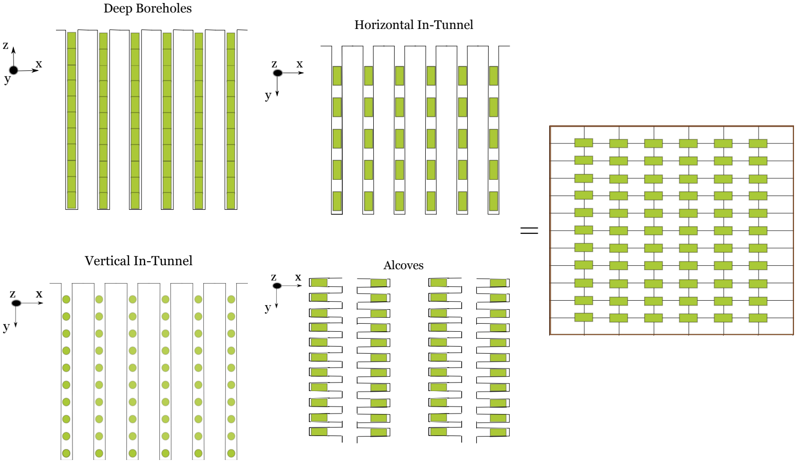

Analytical Model : Geometry

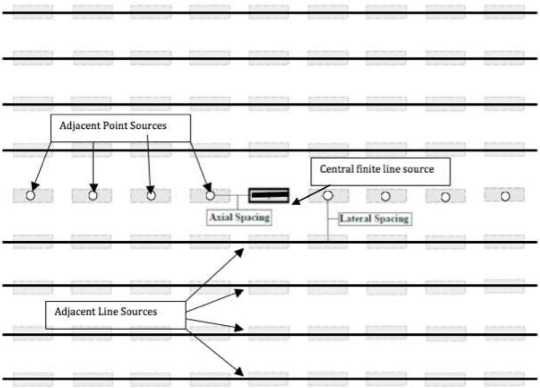

Figure: Vertical, horizontal, alcove, and borehole emplacement layouts can be represented by a line of point sources and adjacent line sources [17].

Analytical Model : Calculation Method

LLNL's model is a MathCAD solution of the transient homogeneous conduction equation,

$$\nabla^2 T = \frac{1}{\alpha}\frac{\partial T}{\partial t}, \tag{1}$$

in which superimposed point and line source solutions approximate the repository layout.

Analytical Model : Calculation Method

The model consists of two conceptual regions, an external region representing the host rock and an internal region representing the waste form, package, and buffer Engineered Barrier System within the disposal tunnel wall.

- Since the thermal mass of the EBS is small in comparison to the thermal mass of the host rock, the internal region may be treated as quasi-steady state.
- The transient state of the temperature at the calculation radius is found with a convolution of the transient external solution with the steady state internal solution.
- The internal and external regions are **approximated** to be a single homogeneous medium.
- The process is then iterated with a one year resolution in order to arrive at a temperature evolution over the lifetime of the repository.

Analytical Model : Calculation Method

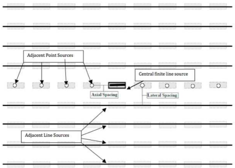

Figure: The central package is represented by a finite line source [17].

The geometric layout of the analytic LLNL model in Figure 14 shows that the central package is represented by the finite line solution

$$T_{line}(t,x,y,z) = \frac{1}{8\pi K_{th}} \int_0^t \frac{q_L(t')}{t-t'} e^{\frac{-\left(x^2+z^2\right)}{4\alpha(t-t')}} \cdot \left[\mathrm{erf}\left[\frac{1}{2}\frac{\left(y+\frac{L}{2}\right)}{\sqrt{\alpha(t-t')}}\right] - \mathrm{erf}\left[\frac{1}{2}\frac{\left(y-\frac{L}{2}\right)}{\sqrt{\alpha(t-t')}}\right]\right] \mathrm{d}t'. \tag{2}$$

Analytical Model : Calculation Method

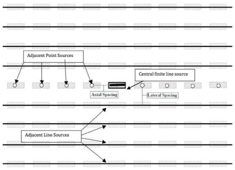

Figure: Adjacent packages are represented as point sources [17].

Adjacent packages within the central tunnel are represented by the point source solution,

$$T_{point}(t, r) = \frac{1}{8K_{th}\sqrt{\alpha}\pi^{\frac{3}{2}}} \int_0^t \frac{q(t')}{(t-t')^{\frac{3}{2}}} e^{\frac{-r^2}{4\alpha(t-t')}} \, \mathrm{d}t'. \tag{3}$$

Analytical Model : Calculation Method

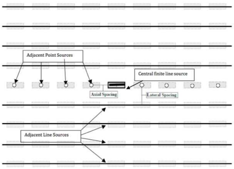

Figure: The non-central disposal tunnels are represented as infinite line sources [17].

Adjacent disposal tunnels are represented by the infinite line source solution,

$$T_{\infty line}(t, x, z) = \frac{1}{4\pi K_{th}} \int_0^t \frac{q_L(t')}{t - t'} e^{\frac{-\left(x^2+z^2\right)}{4\alpha(t-t')}} \tag{4}$$

in infinite homogeneous media, where

$$\alpha = \text{ thermal diffusivity } [m^2 \cdot s^{-1}]$$

$$q(t) = \text{ point heat source}[W]$$

and

$$q_L(t) = \text{ linear heat source}[W \cdot m^{-1}]$$

Superimposed point and line source solutions allow for a notion of the repository layout to be modeled in the host rock.

Numerical Model : SINDA\G Technique

This techinique was originally created for optimal waste loading analysis of YMR by the UFD team at Argonne national lab. It uses the SINDA\G heat transport framework which employs a geometrically precise numerical lumped parameter model.

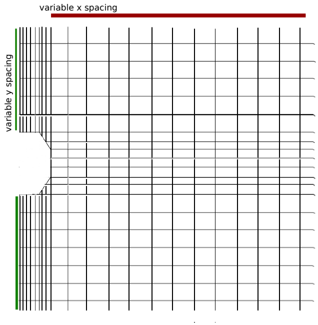

Figure: The geometry of the 2D thermal model can be adjusted by altering tunnel diameter, tunnel spacing, and the vertical distance below the surface.

Numerical Model : Lumped Parameter Technique

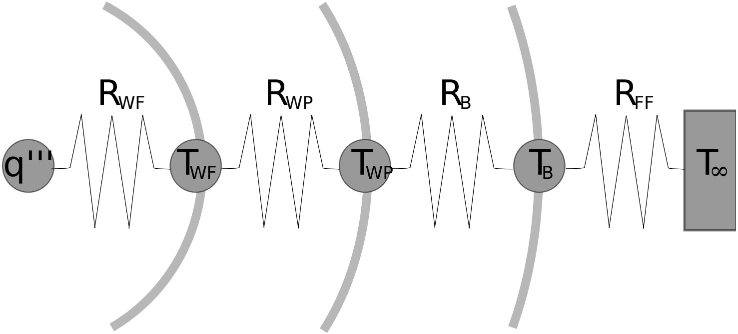

Figure: The lumped parameter analogy used for heat transfer can be applied as a one dimensional approximation to the disposal system concept.

Numerical Model : Calculation Method

The SINDA\G lumped capacitance tool solves a thermal circuit, for which conducting nodes may be of four types corresponding to the four modes of heat transfer. Nodes are connected by conduction, convection, radiation, and mass flow heat transfer links. In the SINDA\G engine, these are represented by

$$R_{rad} = \frac{1}{\sigma F_{ij} A \left[T_i + T_A + T_j + T_A\right]\left[(T_i + T_A)^2 + (T_j + T_A)^2\right]}$$

$$R_{cond} = \frac{L}{K_{th} A}, \; R_{conv} = \frac{1}{hA}, \text{ and } R_{mf} = \frac{1}{\dot{m} c_p} \tag{5}$$

where

$$\begin{aligned}
K_{th} &= \text{ thermal conductivity}[W \cdot m^{-1} \cdot K^{-1}] \\
A &= \text{ area}[m^2] \\
c_p &= \text{ specific heat capacity}[J \cdot K^{-1}] \\
h &= \text{ heat transfer coefficient}[W \cdot m^{-1} \cdot K^{-1}] \\
\dot{m} &= \text{ mass transfer rate}[kg \cdot s^{-1}] \\
T_i &= \text{ lump temperature}[^\circ C] \\
T_A &= \text{ absolute temperature}[^\circ C] \\
F_{ij} &= \text{ radiation interchange factor}[-].
\end{aligned}$$

Numerical Model : SINDA\G Geometries

Two SINDA\G model geometries have been used in this benchmark.

- **Single Drift** In the single drift geometry, there is a distant fixed boundary condition and one waste tunnel is modeled with a continuous, cylindrical heat source of infinite length. The linear heat source in $[\frac{W}{m}]$ is modeled as if it is spread azimuthally over the surface of the drift tunnel.
- **Multiple Drift** As llustrated in Figure 15, an infinite array of identical single-drift heat sources is modeled, by assuming one-half of a storage tunnel with a reflective boundary condition at a vertical plane midway between drifts.

Benchmarking : Single Tunnel Case, Peak Heat

For the single tunnel geometry benchmark, the analytic model gave peak temperatures for all cases run which agreed with the numeric model within $4^{\circ}C$ and, for calculation radii less than 5 meters.

Benchmarking Results for Single Tunnel Scenario

	Peak Temperature Discrepancy $T_{peak,num} - T_{peak,an}$ $[^{\circ}C]$					
Material	Clay $K_{th} = 2.5$ $\alpha = 1.13 \times 10^{-6}$			Salt $K_{th} = 4.2$ $\alpha = 2.07 \times 10^{-6}$		
Years Cooling	10	25	50	10	25	50
R=0.35m	3.0	2.3	1.6	2.0	1.7	1.2
R=0.69m	3.1	2.4	1.6	2.2	1.8	1.3
R=3.46m	2.1	1.9	1.5	2.2	1.7	1.3

Table: Benchmarking in the single tunnel case showed that the peak heat was calculated to be lower and arrived consistently sooner in the analytic (an) model than in the numeric (num) model.

Benchmarking : Single Tunnel Case, Timing

For the single tunnel geometry benchmark, the analytic model consistently reported peak temperature timing within 11 years of the ANL numeric model.

Benchmarking Results for Single Tunnel Scenario

	Peak Heat Timing Discrepancy $t_{peak,num} - t_{peak,an}$ [yr]					
Material	Clay $K_{th} = 2.5$ $\alpha = 1.13 \times 10^{-6}$			Salt $K_{th} = 4.2$ $\alpha = 2.07 \times 10^{-6}$		
Years Cooling	10	25	50	10	25	50
R=0.35m	1	1	1	1	1	3
R=0.69m	2	2	1	2	3	4
R=3.46m	9	7	6	4	2	11

Table: Benchmarking in the single tunnel case showed that the peak heat was calculated to be lower and arrived consistently sooner in the analytic (an) model than in the numeric (num) model.

Benchmarking : Single Tunnel Case, Clay

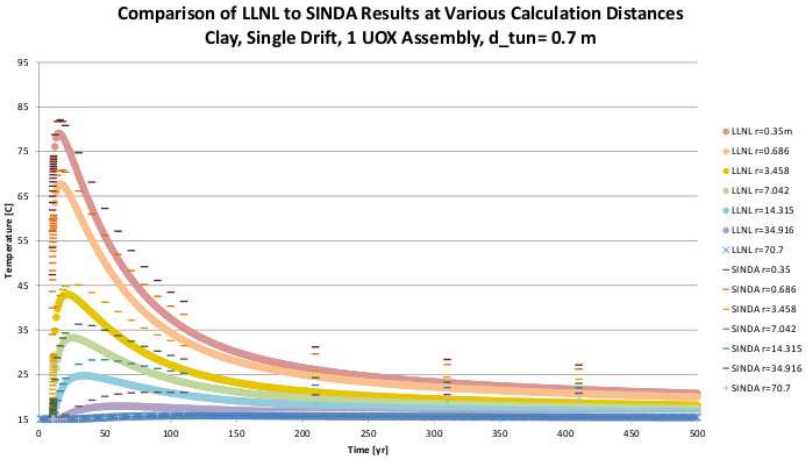

Figure: UOX waste form, 10 years cooling, clay scenario.

Benchmarking : Single Tunnel Case, Salt

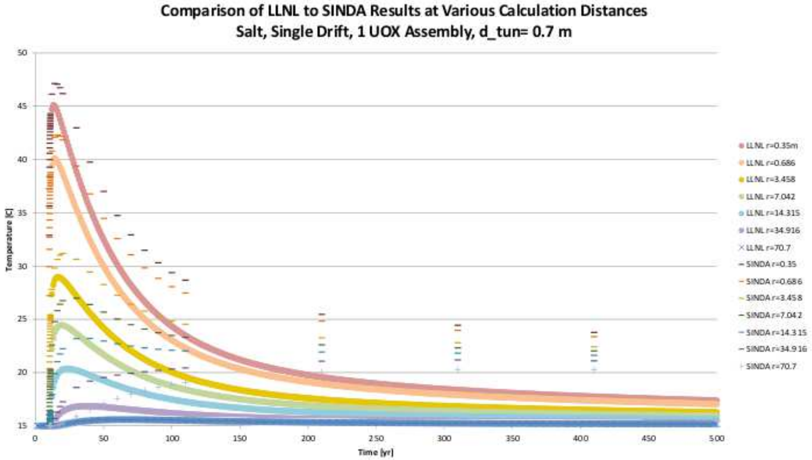

Figure: UOX waste form, 10 years cooling, salt scenario.

Benchmarking : Multiple Tunnel Case

For the multiple tunnel case, in which the numeric model approximated an infinite array of tunnels and the analytic approach modeled 101, the differences between models were slightly greater.

Benchmarking Results for 101 Tunnel Scenario

Material	Clay $K_{th} = 2.5$ $\alpha = 1.13 \times 10^{-6}$		
	Peak Temperature Discrepancy $T_{peak,num} - T_{peak,an}$ $[^\circ C]$		
Years Cooling	10	25	50
R=0.35m	7	4.6	2.1
	Peak Heat Timing Discrepancy $t_{peak,num} - t_{peak,an}$ [yr]		
R=0.35m	-13.5	2	-6

Table: Benchmarking in the multiple tunnel case showed that the peak heat was calculated to be consistently lower in the analytic (an) model and deviated further from the numeric (num) model than did the single tunnel case.

Benchmarking : Summary

In light of the magnitude of uncertainties involved in generically modeling a non-site-specific geologic repository, this sufficiently validated the analytic LLNL model with respect to its goals. The analytic model would seem well-suited for purposes of rapid evaluation of generic geologic repository configurations. The benchmark revealed a notable discrepancy between the two models, however. The time of peak heat arrived consistently sooner and the value of the peak temperature was consistently lower in the homogeneous medium analytic model than in the numeric model.

Outline

Calibration : Goals

The goal of the calibration effort was to improve near field, short time scale results of the analytic model using the numeric model. The EBS responds to

changes in the waste package decay heat more rapidly than the field in the surrounding host rock. This behavior is not taken into account in the analytic model, but is explicitly accounted for in the numeric model.

Calibration : Resistance Factor

The difference in temperature due to the instantaneous transient response in the tunnel is here modeled as ΔT,

$$\Delta T(t) = T_{numeric}(r_t) - T_{analytic}(\frac{D_d}{2}) \tag{6}$$

$$\Delta T(t) = Cq_L(t)\frac{1}{K_{th}}\frac{1}{D_d} \tag{7}$$

where

$$D_d = \text{Distance between drifts}[m]$$
$$r_t = \text{Tunnel wall radius, calculation radius}[m]$$

and

$$C = \text{A coefficient derived from fitting}[m].$$

This allows the capacitive behavior of the model to remain entirely in the analytic model, and embeds the resistive behavior in a purely algebraic calibration. The calibration is valid for all repository configurations which share a tunnel diameter, tunnel spacing, and host rock material.

Calibration : Multiple Tunnel Results

For a clay repository ($K_{th} = 2.5[W \cdot m^{-1} \cdot K^{-1}]$, $\alpha = 1.13 \times 10^{-6}[m^2 \cdot s^{-1}]$), with a tunnel diameter of $0.7m$, the calibration was completed using a fit between a 101 drift analytic scenario and the numeric model with an infinite number of drifts. D_d, the drift spacing, was $30m$ in each case.
A fitting coefficient of $C = 0.0265m$ improves agreement for the clay case with a $0.7m$ tunnel diameter and multiple drifts. The success of the fit decreases for longer cooling times.

100 Tunnel 10 year

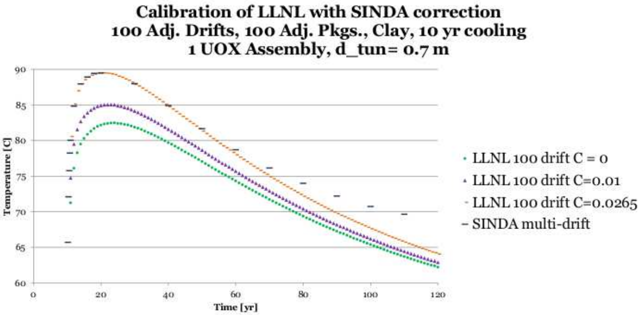

Figure: A multiple drift scenario approximated the inifinite repository scenario run with the SINDA technique.

100 Tunnel 25 year

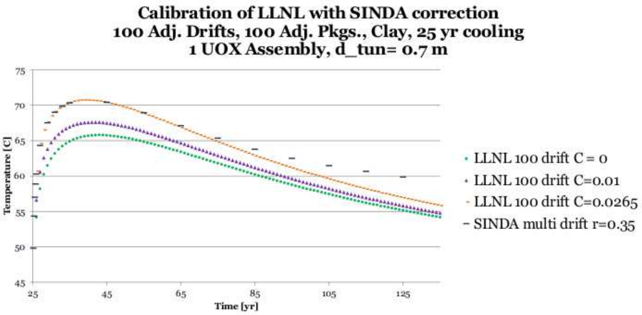

Figure: A multiple drift scenario approximated the inifinite repository scenario run with the SINDA technique.

100 Tunnel 50 year

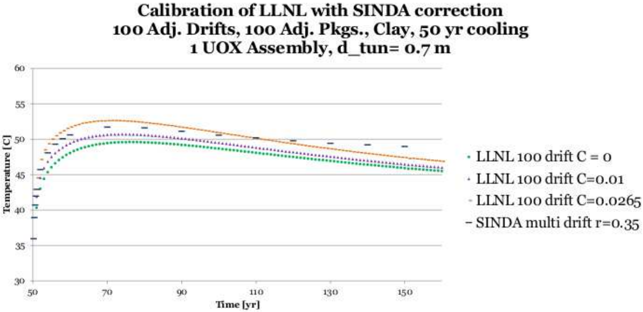

Figure: A multiple drift scenario approximated the inifinite repository scenario run with the SINDA technique.

Calibration : Single Tunnel Fitting Results

A fitting coefficient of $C = 0.01m$ improves agreement for the clay case with a $0.7m$ tunnel diameter and a single tunnel. The success of the fit decreases for longer cooling times.

1 Tunnel 10 year

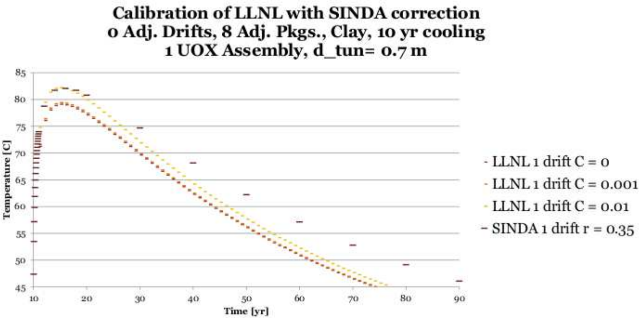

Figure: A single tunnel scenario was compared to the single tunnel repository scenario run with the SINDA technique.

1 Tunnel 25 year

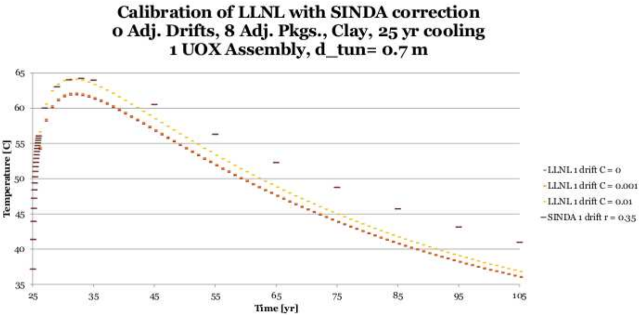

Figure: A single tunnel scenario was compared to the single tunnel repository scenario run with the SINDA technique.

1 Tunnel 50 year

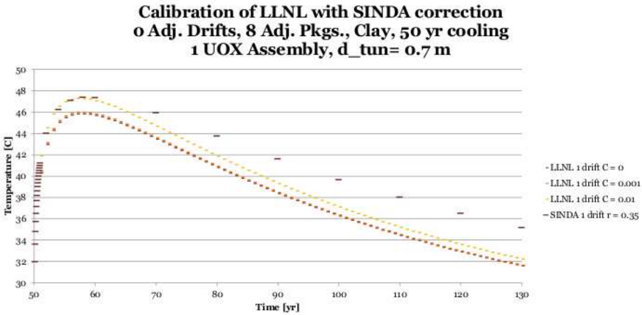

Figure: A single tunnel scenario was compared to the single tunnel repository scenario run with the SINDA technique.

Summary

Benchmarking and calibration of an analytical thermal model against a detailed numerical model showed that the analytical model was accurate within an acceptable range and that it can be adjusted simply using a resistance based calibration technique.

Acknowledgements

This work is supported by the U.S. Department of Energy, Basic Energy Sciences, Office of Nuclear Energy, under contract # DE-AC02-06CH11357.

References I

[1] ANDRA.
Argile: valuation de la faisabilit du stockage gologique en formation argileuse.
Technical report, 2005.

[2] ANDRA.
Granite: valuation de la faisabilit du stockage gologique en formation granite.
Technical report, 2005.

[3] JB Bush.
Economic and technical feasibility study of compressed air storage.
General Electric Company. Office of Conservation, US Energy Research and Development Administration, 1976.

[4] H. S Carslaw and J. C Jaeger.
Conduction of heat in solids.
Oxford: Clarendon Press, 1959, 2nd ed., 1959.

[5] D Clayton, G Freeze, E Hardin, W.M. Nutt, J Birkholzer, H.H. Liu, and S Chu.
Generic disposal system modeling - fiscal year 2011 progress report.
Technical Report FCRD-USED-2011-000184, U.S. Department of Energy, Sandia, NM, August 2011.

References II

[6] S. Gonzales and K. S Johnson.
Shales and other argillaceous strata in the United States.
1985.

[7] Harris Greenberg, James Blink, Massimiliano Fratoni, Mark Sutton, and Amber Ross.
Application of analytical heat transfer models of Multi-Layered natural and engineered barriers in potential High-Level nuclear waste repositories.
In *Waste Management*, Phoenix, AZ, feb 2012.

[8] E Hardin, J Blink, Harris Greenberg, Mark Sutton, Massimo Fratoni, Joe Carter, Mark Dupont, and Rob Howard.
Generic repository design concepts and thermal analysis - 8.8.2011 draft.
Technical Report FCRD-USED-2011-000143, Department of Energy Office of Used Fuel Disposition, Sandia, August 2011.

[9] L. Johnson, B. Kunz, C. Frei, Nagra, and Projekt Opalinuston.
Project Opalinus Clay: Safety Report: Demonstration of Disposal Feasibility for Spent Fuel, Vitrified High-level Waste and Long-lived Intermediate-level Waste (Entsorgungsnachweis).
Nagra, National cooperative for the Disposal of Radioactive Waste, 2002.

References III

[10] L. H. Johnson and Nagra.
Calculations of the temperature evolution of a repository for spent fuel, vitrified high-level waste and intermediate level waste in Opalinus Clay.
Nagra, 2002.

[11] Svensk karnbranslehantering AB.
Long-term Safety for KBS-3 Repositories at Forsmark and Laxemara First Evaluation: Main Report of the SR-Can Project.
SKB, 2006.

[12] J. Li, M. Nicholson, W. C Proctor, M. S Yim, and D. McNelis.
Examining repository loading options to expand yucca mountain repository capacity.
In *Proceedings of GLOBAL*, page 519525, 2007.

[13] NewScientist.
Where should the US store its nuclear waste? - 06 april 2011 - new scientist.
http://www.newscientist.com/article/dn20339-where-should-the-us-store-its-nuclear-waste.html, April 2011.

[14] M. A Nicholson.
Thermal Loading and Uncertainty Analysis of High Level Waste in Yucca Mountain.
North Carolina State University., 2007.

References IV

[15] PTC.
PTC mathcad engineering calculations software.
http://www.ptc.com/product/mathcad/, 2010.

[16] T. E Radel.
Repository modeling for fuel cycle scenario analysis.
University of WisconsinMadison, 2007.

[17] M. Sutton, J. Blink, M. Fatoni, H. Greenberg, and A. Ross.
Investigations on repository near field thermal modeling.
Technical Report LLNL-TR-491099, Lawrence Livermore National Laboratory, July 2011.

[18] W. von Lensa, R. Nabbi, and M. Rossbach.
RED-IMPACT Impact of Partitioning, Transmutation and Waste Reduction Technologies on the Final Nuclear Waste Disposal.
Forschungszentrum J\lich, 2008.